CrossMark

Preparation and characterization of all-oxide CuFeO$_2$:Zn/ZnO:Al transparent heterojunction diode by using all-chemical solution deposition

M. Asemi[1] · H. Mameghani[1] · M. Ghanaatshoar[1]

Abstract Transparent p-n heterojunction thin-film diodes have been fabricated through an all-chemical solution deposition as a low-cost and large-scale method. In this order, we firstly studied the structural, optical and electrical properties of fabricated n-ZnO:Al and p-CuFeO$_2$:Zn layers. The deposited ZnO:Al thin film showed a transmission more than 90 % in the visible range, and its smooth surface provided a suitable substrate for preparation of the diode. The current–voltage characteristic of the CuFeO$_2$:Zn/ZnO:Al p-n junction demonstrated rectifying property. The diode with a total thickness of 1240 nm exhibited around 60 % optical transparency in the visible region which makes it suitable for invisible electronic and optoelectronic devices.

Graphical Abstract
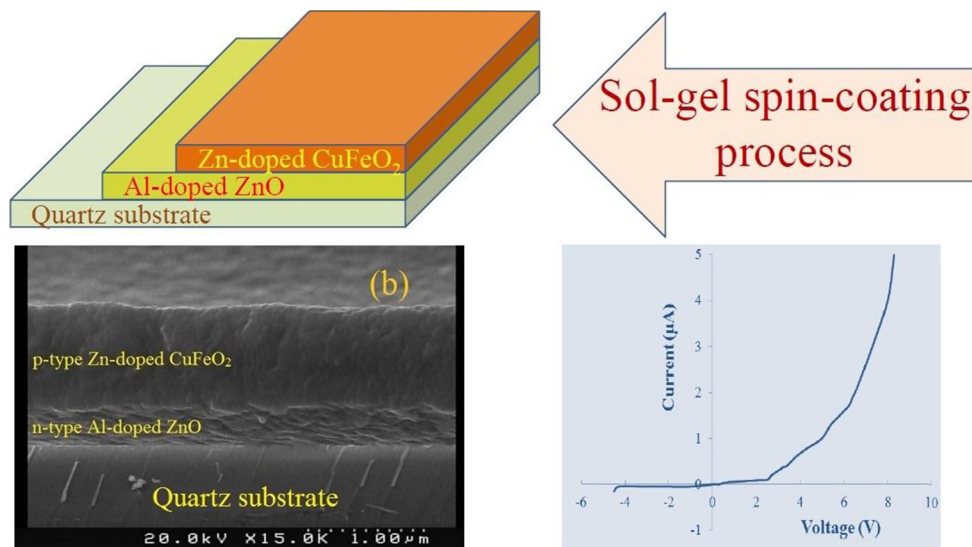
Keywords All-chemical solution deposition · Transparent diode · p-n junction

1 Introduction

Transparent conducting oxides (TCOs) are used in optoelectronics due to their wide band gap and also high conductivity [1]. Transparent optoelectronic devices such as

✉ M. Ghanaatshoar
m-ghanaat@sbu.ac.ir

1 Laser and Plasma Research Institute, Shahid Beheshti University, G.C., Evin, 1983969411 Tehran, Iran

functional windows, transparent or semitransparent solar cells and light-emitting diodes require both n-type and p-type transparent materials [2]. n-type TCOs such as Sn-doped In_2O_3 (ITO), Al-doped ZnO (AZO) and F-doped SnO_2 (FTO) are well known and have been studied for many years [3]. However, p-type TCOs such as $CuAlO_2$, $CuCrO_2$ and $CuGaO_2$ have only recently been investigated [4]. The conductivity of transparent p-type conductors is usually lower than that of n-type TCOs because of lower mobility of holes in p-type TCOs compared to that of electrons in n-type ones.

Al-doped zinc oxide is one of the n-type oxide semiconductors with direct wide band gap (3.37 eV at room temperature) which is used in fabrication of optoelectronic devices in the blue and ultraviolet regions. AZO has high electrical conductivity and show high optical transparency in the visible region [5, 6]. It has attracted interest as a transparent electrode for thin-film solar cells, light-emitting diodes and gas sensors. Similarly, AMO_2 (A = Pd, Cu and M = Al, In, Fe, Cr) is a noble metal oxide alike n-type TCOs with the difference that the AMO_2 TCO has p-type conductivity [7, 8]. For the first time, Kawazoe et al. reported the synthesis of p-type delafossite $CuAlO_2$ thin films by pulsed laser deposition that possess both high electrical conductivity and transparency in visible region [9]. $CuFeO_2$ is another delafossite-type TCO with p-type conductivity and good electro-optical properties. The crystal structure of $CuFeO_2$ belongs to the space group $R\bar{3}$ m with $a_h = 3.03$ Å and $c_h = 17.09$ Å in the hexagonal description [10, 11]. This TCO has been intensively studied due to its various electrical, optical and magnetic applications. For instance, antiferromagnetic structure and field-induced magnetic-phase transitions of $CuFeO_2$ were recognized by Terada et al. [12]. $CuFeO_2$ thin films were fabricated on glass substrate by RF magnetron sputtering, and p-type conductivity of $CuFeO_2$ was studied using thermopower measurements [13]. The pulsed laser deposition method was also used to fabricate $CuFeO_2$ thin films on amorphous glass substrates by Choi et al. [10]. In addition, Chen and Wu constructed transparent and conductive $CuFeO_2$ thin films by using sol–gel method [11].

As mentioned above, one application of p- and n-type TCOs is in fabricating transparent thin-film diodes. The first work on transparent heterojunction was reported by Sato et al. [14] on semitransparent p-NiO/i-NiO/i-ZnO/n-ZnO heterojunction with 20 % visible transparency. Afterward, various groups reported the fabrication of p-i-n and p-n homojunction and heterojunction diodes with proper electro-optical properties for potential application in invisible electronics. Most of fabricated diode structures are heterojunctions such as $p-SrCu_2O_2/n-ZnO$ [15], $p-SrCu_2O_2/i-ZnO/n-ZnO$ [16], $p-CuY_{1-x}Ca_xO_2/n-Zn_{1-x}Al_xO$ [17], $p-CuY_{1-x}Ca_xO_2/i-ZnO/n-ITO$ [18], $CuCrO_2:Mg/ZnO$ [1, 19].

As fabricated homojunction diodes, we can also point to $p-CuIn_{1-x}Ca_xO_2/n-CuIn_{1-x}SnO_2$ [20], p-ZnO:P/n-ZnO [21] and p-ZnO:As/n-ZnO [22]. In order to fabricate thin-film diodes, each layer is deposited on the substrate by one of the thin-film deposition methods such as pulsed laser deposition, RF magnetron sputtering, reactive evaporation and thermal evaporation [8, 23–25] and chemical solution deposition [11, 26, 27]. The physical methods of preparing transparent diodes are complex, expensive and, moreover, need high vacuum. On the contrary, the chemical solution methods of preparing multilayers have cost-reduction advantage [11].

In this paper, we report the all-chemical solution fabrication of a TCO diode based on $p-CuFeO_2:Zn$. The n-type semiconductor utilized to construct the transparent heterojunction is Al-doped ZnO. Prior to create this TCO diode, we fabricate and characterize n-type ZnO:Al and p-type $CuFeO_2:Zn$ thin layers. The diode I–V characteristic of $CuFe_{0.95}Zn_{0.05}O_2/Zn_{0.99}Al_{0.01}O$ heterojunction verifies the ability of chemical solution deposition method to create diode structure.

2 Experimental details

To prepare $Zn_{1-x}Al_xO$ thin film, $Zn(CH_3COO)_2 \cdot 2H_2O$ and $Al(NO_3)_3 \cdot 9H_2O$ were used as starting materials. Furthermore, 2-methoxyethanol and monoethanolamine were used as solvent and stabilizer, respectively. The concentration of Zn metallic ion was 0.7 molar, and the molar ratio between ethanolamine and metallic ions (Zn + Al) was kept at 1. Firstly, starting materials were dissolved in the solvent. Then, monoethanolamine was added to the solution as a stabilizer. The mixed solution was stirred in a magnetic stirrer at 60 °C for 2 h to obtain a clear and transparent yellow solution. The resultant solution was aged for 48 h at room temperature.

For film preparation, the quartz substrate was firstly cleaned by acetone and ethanol in an ultrasonic bath before film deposition. The ZnO:Al solution was dropped onto quartz substrate, which was rotated at 3000 rpm for 30 s by using a Backer Viera Trading SC-410 spincoater. After deposition, the thin films were dried at 500 °C for 15 min in an air furnace to evaporate the solvent and organic residuals [28]. This process was repeated for six times to reach a desired thickness. Then, the obtained ZnO:Al thin films were annealed in a vacuum furnace (with a pressure of 10^{-5} mbar) at 500 °C for 1 h [29].

For fabrication of $CuFeO_2:Zn$ thin films, we used $Cu(CH_3OOH)_2 \cdot H_2O$, $Fe(NO_3)_3 \cdot 9H_2O$ and $Zn(CH_3COO)_2 \cdot 2H_2O$ as starting materials. Similarly, 2-methoxyethanol and monoethanolamine were used as solvent and stabilizer, respectively. The concentration of the solution was 0.2 molar in respect of Cu metallic ions. Furthermore, the molar ratio between Cu and Fe + Zn was kept at 1. The
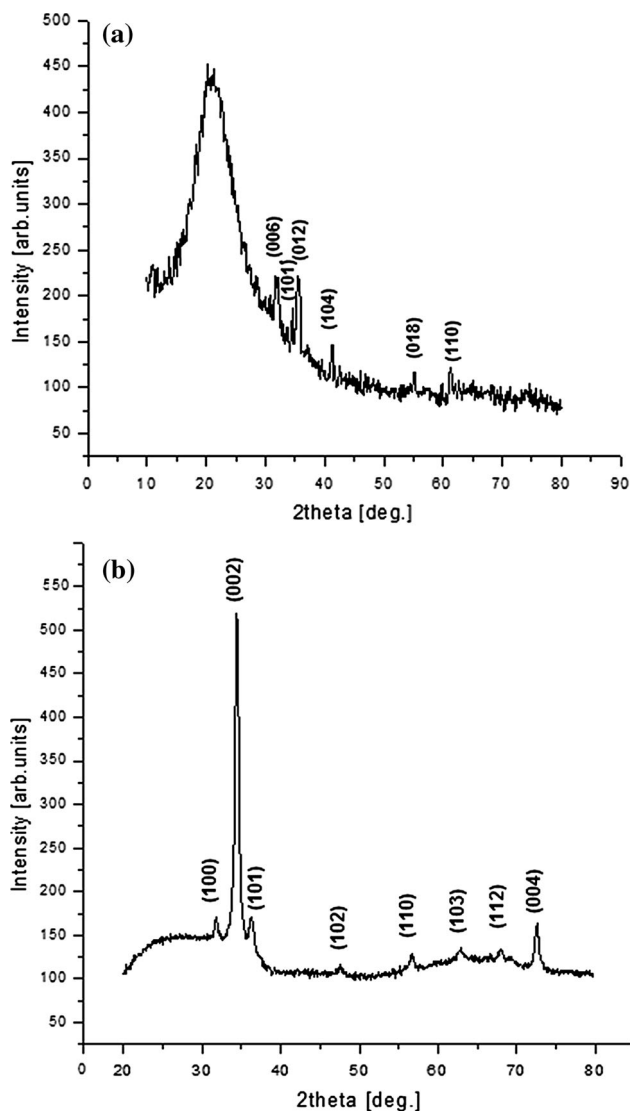
Fig. 1 XRD patterns of **a** CuFe$_{0.95}$Zn$_{0.05}$O$_2$ single layer annealed at 800 °C in flowing argon gas (purity 99.99 %) atmosphere for 1 h and **b** Zn$_{0.99}$Al$_{0.01}$O single layer annealed in a vacuum furnace (with a pressure of 10^{-5} mbar) at 500 °C for 1 h

resulting solution was stirred at 60 °C for 6 h to obtain a homogenous and transparent solution. Then, the precursor sol was dropped onto ZnO:Al/quartz film which was rotated at 2500 rpm for 30 s and then the resultant film was dried in the air furnace at 400 °C for 20 min. This process was repeated for six times to increase the film thickness. Finally, the bilayers were annealed at 800 °C in flowing argon gas (purity 99.99 %) atmosphere for 1 h [11].

The morphology and structural properties of the single layers and the bilayers were analyzed by X-ray diffraction (XRD), field emission scanning electron microscopy (FESEM) and atomic force microscopy (AFM). In addition, energy-dispersive X-ray spectroscopy (EDX) was used for analyzing Al and Zn distribution in AZO and

CuFeO$_2$ thin films, respectively. Moreover, optical properties were studied by UV–Vis–NIR spectrometry and we used the Hall effect measurement, four-probe point and two-probe point techniques to investigate the electrical properties of the layers. The contacts for electrical measurements were provided by using alligator clips.

3 Results and discussion

A heterojunction with diodic character should comprise proper n- and p-type semiconducting layers. Therefore, we firstly studied the structural, electrical and optical properties of n- and p-type layers. Then, the p-n heterojunction diode was fabricated and its properties were investigated. Regarding the scientific reports and our experience, we focused on the layers with nominal composition of Zn$_{0.99}$Al$_{0.01}$O and CuFe$_{0.95}$Zn$_{0.05}$O$_2$ to construct the diode [30]. For simplicity, hereafter we label Zn$_{0.99}$Al$_{0.01}$O n-type layer as AZO and CuFe$_{0.95}$Zn$_{0.05}$O$_2$ p-type layer as CFZO.

The XRD spectra of the prepared AZO and CFZO single layers deposited on quartz substrates are shown in Fig. 1. These patterns indicate that the AZO thin film possesses a polycrystalline ZnO with the hexagonal wurtzite structure and no signature of any impurity (JCPDS# 001-1136). Similarly, the diffraction peaks of CuFeO$_2$ are observed for the CFZO single layer without any extra phase (JCPDS# 74-1953). The XRD pattern of the CFZO illustrates that it is a polycrystalline thin film with a rhombohedral crystalline structure. Though no preferential crystalline direction is observed for the CFZO thin film, the AZO layer shows such a direction. The average crystallite size for (002) preferential orientation is determined by the Debye–Scherrer equation as 19 nm [31]. Similar results and crystallite size have been reported for Al-doped ZnO thin films by Ding et al. and Lin et al. [30, 32].

The energy-dispersive X-ray (EDX) spectra of CFZO and AZO single layers are shown in Fig. 2. According to this figure, the chemical composition ratio of CFZO thin film is Cu: 26.59, Fe: 17.48, O: 51.11 and Zn: 4.82. This set approximately corresponds to the molar ratio of Cu/ Fe + Zn/ O (1:1:2). Similarly, the chemical composition of AZO thin film is Zn: 58.95, O: 39.72 and Al: 1.33. The slightly oxygen stoichiometry deviation in AZO thin film is due to the heat treatment in Ar atmosphere. It is well known that the heat treatment in vacuum or under an inert-gas ambient atmosphere causes the formation of oxygen vacancies and Zn interstitials sites.

The surface morphology of the prepared CFZO and AZO thin films has been observed by FESEM. Figure 3 shows that the surface of deposited films has homogeneous, continuous and dense structures. The average grain size of

Fig. 2 EDX spectroscopy of **a** $CuFe_{0.95}Zn_{0.05}O_2$ single layer annealed at 800 °C in flowing argon gas atmosphere for 1 h and **b** $Zn_{0.99}Al_{0.01}O$ single layer annealed in a vacuum furnace (with a pressure of 10^{-5} mbar) at 500 °C for 1 h
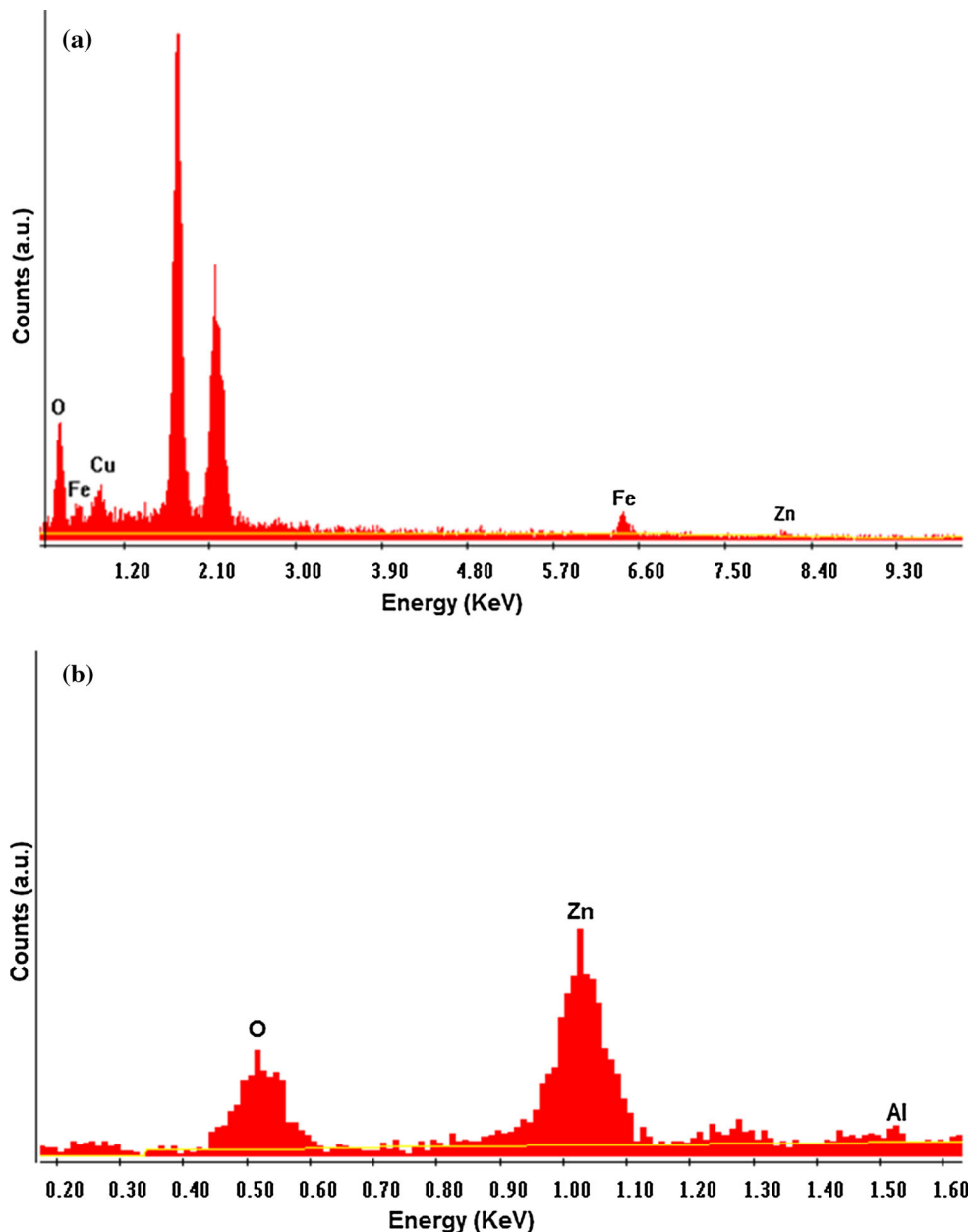
$CuFe_{0.95}Zn_{0.05}O_2$ and $Zn_{0.99}Al_{0.01}O$ thin films is typically around 62 and 39 nm, respectively. Figure 4 shows the AFM images of the films. The root mean square (RMS) roughness of the CFZO single layer is about 62.4 nm. In contrast, the surface of $Zn_{0.99}Al_{0.01}O$ is smooth, regular and uniform. The roughness of this thin film is around 10.1 nm. The smooth surface of AZO/quartz makes it a good substrate for preparation of CFZO/AZO/quartz heterojunction.

Figure 5a shows the transmission spectra of the thin films deposited onto the quartz substrate. As can be seen, the transmittance of CFZO thin film is around 25–50 % in the visible range. This result is similar to that of $CuFeO_2$ prepared by Chen et al. [11]. Transmittance of $CuFeO_2$ is lower than those of $CuAlO_2$ [16] and $CuCrO_2$ [30] delafossites which is due to d–d transition of iron [11]. The transmittance of AZO thin film is also seen in Fig. 5 which is higher than 90 % in the visible region. For this reason, AZO thin film is appropriate as a window layer in diode fabrication. We can determine the optical band gap of the layers by using the transmission spectra. The electron excitation from the valance to the conduction band requires energy around the band gap energy. The absorption coefficient relates to the photon energy hv through $(\alpha hv)^2 = A(hv - E_g)$, where A is a constant and E_g is the optical band gap energy [33]. As seen in Fig. 5b, the plot of $(\alpha hv)^2$

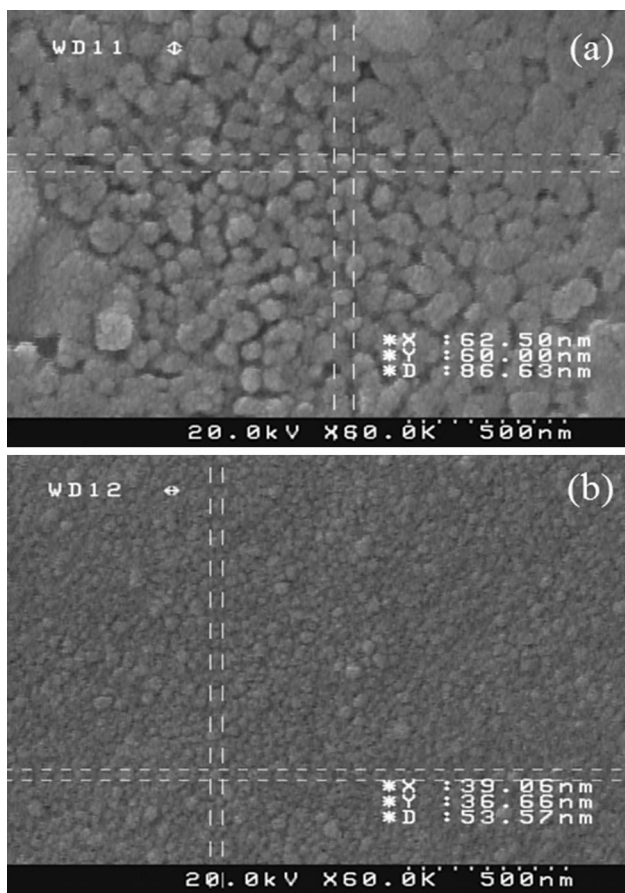**Fig. 3** SEM images of **a** CuFe$_{0.95}$Zn$_{0.05}$O$_2$ single layer on quartz substrate annealed at 800 °C in flowing argon gas atmosphere for 1 h, and **b** Zn$_{0.99}$Al$_{0.01}$O single layer annealed in a vacuum furnace at 500 °C for 1 h

against $h\nu$ near the fundamental absorption edge determines the direct energy band gap [34] of CFZO which is about 3.11 eV. The direct band gap of AZO is also determined as 3.3 eV. These materials with band gaps higher than 3.0 eV are suitable for fabrication of transparent diodes.

The n-type conductivity of AZO single layer and p-type conductivity of CFZO single layer have been confirmed by using the hot-probe technique. We have also used the Hall effect setup to measure the carrier concentration and charge carrier mobility of the prepared thin films. The carrier concentration and mobility of the AZO thin film are 2.8×10^{19} cm^{-3} and 3.27 cm^2/Vs, respectively. These values for the CFZO thin film are 1.2×10^{19} cm^{-3} and 2.6 cm^2/Vs, respectively. To calculate the conductivity of the thin films, we have used $\sigma = en\mu$ equation in which σ, e, n and μ are conductivity, electron charge magnitude, carrier concentration and mobility of carriers, respectively. The conductivity has been obtained as 14.69 S.cm^{-1} for the AZO thin layer and 4.9 S.cm^{-1} for the CFZO single layer. The electrical conductivity in Al-doped ZnO films is known to be essentially due to the substitution of the Al^{3+} ions for the Zn^{2+} sites, Zn and Al interstitial atoms and oxygen vacancies [35]. The conductivity of the produced CFZO thin film is higher than that of CuFeO$_2$ thin films fabricated by Chen et al. [11]. The improvement in electrical properties of CuFeO$_2$ by doping of divalent cations has also already been reported. When Zn^{2+} is substituted for Fe^{3+}, because of creating the hole, the p-type electrical conductivity is improved [36].
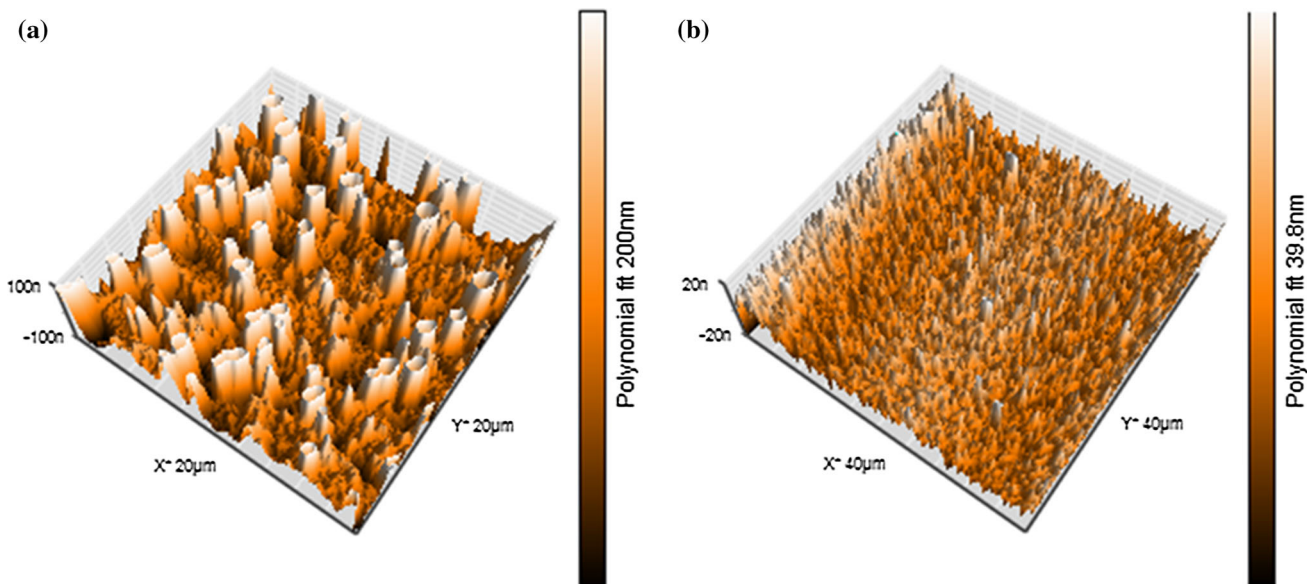

Fig. 4 AFM images of **a** CuFe$_{0.95}$Zn$_{0.05}$O$_2$ single layer annealed at 800 °C in flowing argon gas atmosphere for 1 h, and **b** Zn$_{0.99}$Al$_{0.01}$O single layer on quartz substrate annealed in a vacuum furnace at 500 °C for 1 h
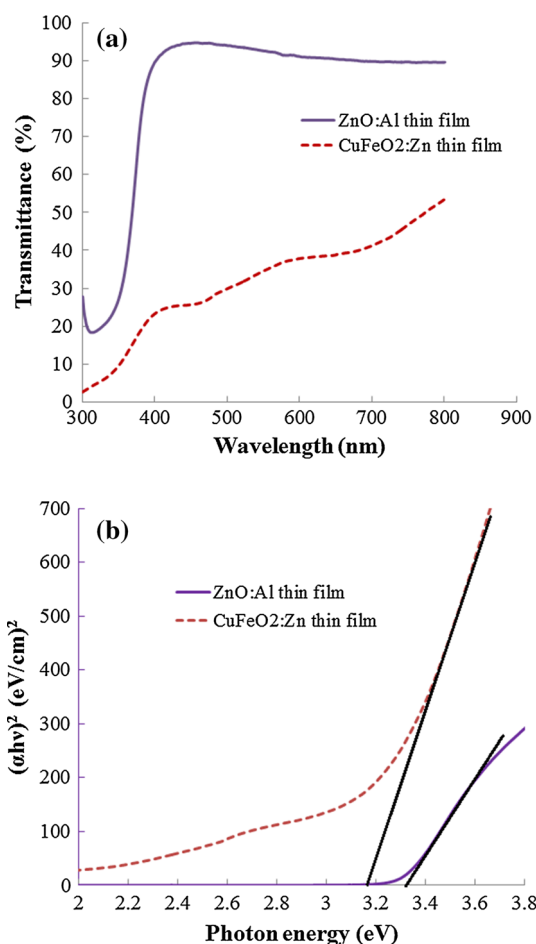
Fig. 5 a Transmittance spectra and **b** plots of $(\alpha h v)^2$ versus photon energy of the $CuFe_{0.95}Zn_{0.05}O_2$ single layer annealed at 800 °C in flowing argon gas atmosphere for 1 h and the $Zn_{0.99}Al_{0.01}O$ single layer annealed in a vacuum furnace at 500 °C for 1 h

Having achieved transparent CFZO and AZO single layers, we fabricate the all-oxide p-n heterojunction diode on quartz substrate (19 mm × 19 mm) by using the all-chemical solution deposition approach. For preparation of heterojunction, firstly AZO thin film is fabricated on quartz substrate and annealed in a vacuum furnace to increase its conductivity. According to Fig. 3, this treatment makes the surface of the AZO film so smooth for subsequent deposition of the p-layer. The smooth surface of the AZO can prevent the interdiffusion of the AZO and CFZO layers. After preparing the AZO layer, the CFZO thin film is deposited on the surface of the annealed AZO/quartz substrate. Finally, the prepared CFZO/AZO/quartz heterojunction is annealed at 800 °C in flowing argon gas (purity 99.99 %) atmosphere for 1 h to obtain the delafossite structure of CFZO layer. Figure 6a shows the XRD pattern of the fabricated p-n heterojunction. As can be seen from this figure, the refraction peaks of CFZO have been obtained besides the peaks of the AZO. The XRD pattern of the heterojunction shows that the intensity of CFZO peaks has increased in comparison with
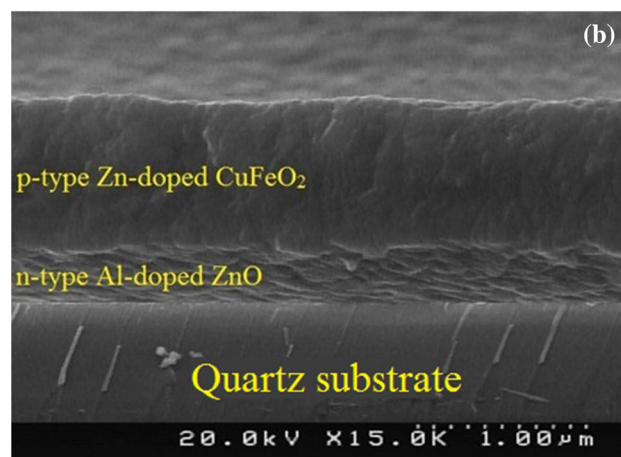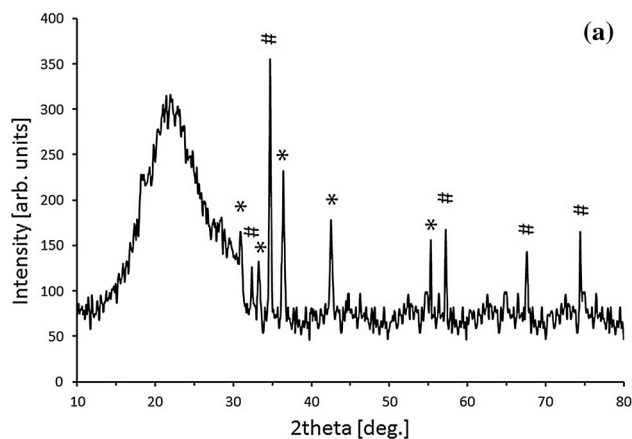

Fig. 6 a XRD pattern and **b** cross-sectional FESEM image of the fabricated p-n junction. The AZO layer in this heterojunction has been exposed to two-step annealing. Firstly, at 500 °C for 1 h in vacuum and then (in the presence of the overlayer), for 1 h at 800 °C in flowing argon gas
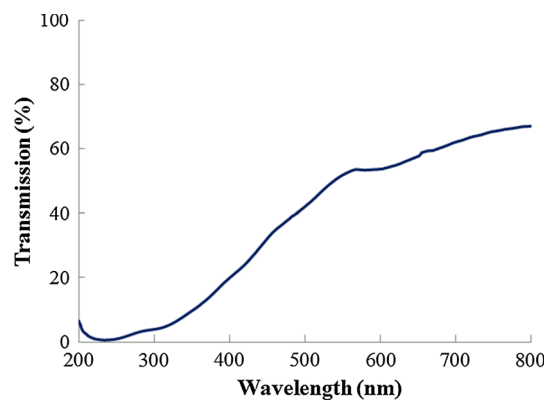

Fig. 7 Transmittance of $p\text{-}CuFe_{0.95}Zn_{0.05}O_2/n\text{-}Zn_{0.99}Al_{0.01}O$/quartz heterojunction

that of the CFZO single layer (see Fig. 1a). The exhibited cross-sectional FESEM image of CFZO/AZO heterojunction on quartz substrate in Fig. 6b reveals that the interface of CFZO/AZO is smooth. From the cross-sectional FESEM
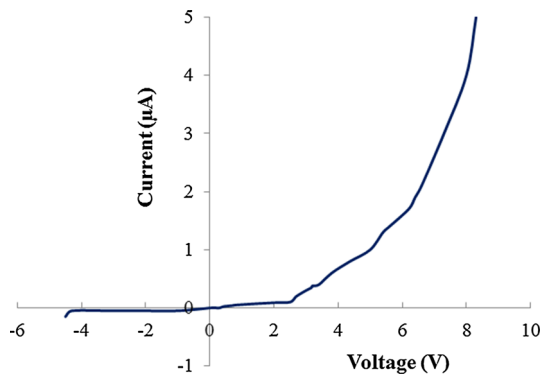
Fig. 8 I–V curve of n-$Zn_{0.99}Al_{0.01}O$/p-$CuFe_{0.95}Zn_{0.05}O_2$ heterojunction

image of the CFZO/AZO heterojunction, the thicknesses of AZO and CFZO layers are estimated as around 320 and 920 nm, respectively.

Figure 7 shows the optical spectrum of $CuFe_{0.95}Zn_{0.05}O_2$/$Zn_{0.99}Al_{0.01}O$ heterojunction. The transmission of heterojunction diode with thickness of 1240 nm is around 55 % at 550 nm which is higher than that of a CFZO single layer. The increase of transmittance in comparison with the CFZO single layer can be ascribed to the interference of light at CFZO/AZO and AZO/quartz interfaces. Similar interference effect was observed for n^+-ZnO/n-ZnO/p-$CuCrO_2$:Mg/ITO p-n junction prepared by pulsed laser deposition by Tonooka et al. [19]. The current–voltage characteristic of the p-n heterojunction has been measured by four-probe setup. As seen in Fig. 8, the nonlinear I–V curve confirms the rectifying property of the created diode. By forward bias measurement, we find the maximum current at 8 V as 5 μA. Moreover, the leakage current is obtained around 50 nA by reverse bias. The reverse breakdown voltage for bilayer structure is around 4 V. The rectifying character accompanied by the optical transparency of the constructed diode verifies the potential of the sol–gel method in producing transparent diodes.

4 Conclusions

In summary, we assembled the p-n heterojunction based on $CuFe_{0.95}Zn_{0.05}O_2$ and $Zn_{0.99}Al_{0.01}O$ thin films on quartz substrate by using sol–gel and spin-coating techniques. It was observed from the experimental results that the AZO thin film is highly transparent having a very smooth surface in comparison with the CFZO thin film. Due to this reason, the AZO coated on quartz was employed as the substrate for deposition of CFZO thin film. Then, the electro-optical properties of the constructed $CuFe_{0.95}Zn_{0.05}O_2$/$Zn_{0.99}Al_{0.01}O$ heterojunction confirmed that the fabricated p-n heterojunction has

rectifying behavior and a transmittance of light around 55 % at the wavelength of 550 nm.

References

1. Baydogan N, Karacasu O, Cimenoglu H (2012) J Sol–Gel Sci Technol 61:620
2. Deng Z, Fang X, Wu S, Dong W, Shao J, Wang S, Lei M (2014) J Sol–Gel Sci Technol 71:297
3. Begum NJ, Ravichandran K (2013) J Phys D Appl Phys 74:841
4. Li G, Zhu X, Lei H, Jiang H, Song W, Yang Z, Dai J, Sun Y, Pan X, Dai S (2010) J Sol–Gel Sci Technol 53:641
5. Tate J, Jayaraj MK, Draeseke AD, Ulbrich T, Sleight AW, Vanaja KA, Nagarajan R, Wager JF, Hoffman RL (2002) Thin Solid Films 411:119
6. Benhaliliba M, Benouis CE, Aida MS, Yakuphanoglu F, Juarez AS (2010) J Sol–Gel Sci Technol 55:335
7. Scanlon DO, Watson GW (2011) J Mater Chem 21:3655
8. Jayalakshmi V, Murugan R, Palanivel B (2005) J Alloys Compd 388:19
9. Kawazoe H, Yasukawa M, Hyodo H, Kurita M, Yanagi H, Hosono H (1997) Nature 389:939
10. Choi DH, Moon SJ, Hong JS, An SY, Shim IB, Kim CS (2009) Thin Solid Films 517:3987
11. Chen HY, Wu JH (2012) Thin Solid Films 520:5029
12. Terada N, Tanaka Y, Tabata Y, Katsumata K, Kikkawa A, Mitsuda S (2006) J Phys Soc Jpn 75:113702
13. Omeiri S, Bellal B, Bouguelia A, Bessekhouad Y, Trari M (2009) J Solid State Electrochem 13:1395
14. Sato H, Minami T, Takata S, Yamada T (1993) Thin Solid Films 236:27
15. Hosono H, Ohta H, Hayashi H, Orita M, Hirano M (2002) J Cryst Growth 496:237
16. Ohta H, Orita M, Hirano M (2001) J Appl Phys 89:5720
17. Jayaraj MK, Draeseke AD, Tate J, Sleight AW (2001) Thin Solid Films 397:244
18. Hoffman RL, Wager JF, Jayaraj MK, Tate J (2001) J Appl Phys 90:5763
19. Tonooka K, Kikuchi N (2006) Thin Solid Films 515:2415
20. Yanagi H, Ueda K, Ohta H, Orita M, Hirano M, Hosono H (2001) Solid State Commun 121:15
21. Aoki T, Hatanaka Y, Look DC (2000) Appl Phys Lett 76:3257
22. Hwang DK, Bang KH, Jeong MC, Myoung JM (2003) J Cryst Growth 254:449
23. Lan W, Cao WL, Zhang M, Liu XQ, Wang YY, Xie EQ, Yan H (2009) J Mater Sci 44:1594
24. Kim SY, Lee JH, Kim JJ, Heo YW (2012) Curr Appl Phys 12:123
25. Dong P, Zhang M, Dong G, Zhao X, Yan H (2008) J Electrochem Soc 155:319
26. Chiu SH, Huang JCA (2013) Surf Coat Technol 231:239
27. Xu L, Li X (2010) J Cryst Growth 312:851
28. Sengupta J, Sahoo RK, Mukherjee CD (2012) Mater Lett 83:84
29. Lin KM, Tsai P (2007) Mater Sci Eng B 139:81
30. Ding J, Chen H, Zhao X, Ma S (2010) J Phys Chem Solids 71:346
31. Asemi M, Ghanaatshoar M (2014) J Sol–Gel Sci Technol 70:416
32. Lin KM, Chen HC, Chen YY, Chou KY (2010) J Sol–Gel Sci Technol 55:369
33. Jiang HF, Zhu XB, Lei HC, Li G, Yang ZR, Song WH, Dai JM, Sun YP, Fu YK (2011) J Alloys Compd 509:1768
34. Caglar Y, Caglar M, Ilican S (2012) Curr Appl Phys 12:963
35. Deng Z, Fang X, Wu S, Zhao Y, Dong W, Shao J, Wang S (2013) J Alloys Compd 577:658
36. Zheng SY, Jiang GS, Su JR, Zhu CF (2006) Mater Lett 60:3871